NISTIR 6588

FIFTEENTH MEETING OF THE UJNR PANEL ON FIRE RESEARCH AND SAFETY MARCH 1-7, 2000

VOLUME 1

Sheilda L. Bryner, Editor

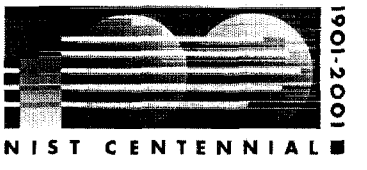

National Institute of Standards and Technology
Technology Administration, U.S. Department of Commerce

NISTIR 6588

FIFTEENTH MEETING OF THE UJNR PANEL ON FIRE RESEARCH AND SAFETY MARCH 1-7, 2000

VOLUME 1

Sheilda L. Bryner, Editor

November 2000

U. S. Department of Commerce
Norman Y. Mineta, Secretary
Technology Administration
Dr. Cheryl L. Shavers, Under Secretary of Commerce for Technology
National Institute of Standards and Technology
Raymond G. Kammer, Director

Fire Safe Materials Project at NIST

Takashi Kashiwagi, Kathryn M.Butler, and Jeffery W. Gilman
Building and Fire Research Laboratory
National Institute of Standards and Technology
Gaithersburg, MD 20899-8652

Abstract

The results of two studies, which are parts of Fire Safe Materials Project at the National Institute of Standards and Technology (NIST), are presented. One of them is a study of the effects on gasification rates of the addition of silica particles to thermoplastics as flame retardant additives; the other is the development of a gasification model of thermoplastics including the growth and transport of bubbles through the molten polymer that forms on the heated surface.

1. Introduction

The Fire Safe Materials Project is one of the major products in the Building Fire Research Laboratory (BFRL) at NIST. The objectives of this project are: (1) to develop new environmentally-friendly flame retardant principles and fire performance prediction capabilities for the U.S. plastics industry. Industry must be assured that modifications to their products will manifest the intended fire performance without significant reduction of (or even with improvement of) their physical properties. And (2) to enable new/improved U.S. products for domestic & international markets, including evaluation of their economic impacts.

This project consists of five different parts. They are focused on: new flame retardant principles, condensed phase processes, gas phase modeling, characterization of physical properties, and the economics of fire safe materials. The study of new flame retardant principles aims to develop and demonstrate successful application of new flame retardant principles for reducing flammability of commodity polymers and also to understand the flame retardant mechanism. Since polymer-clay-nanocomposites, as one of new flame retardant approaches, with polyamid 6 (PA6), polypropylene (PP), and polystyrene (PS), were presented in the 14th Joint Panel Meeting of the United States-Japan Natural Resource (UJNR) Panel on Fire Research and Safety, a brief discussion will be made of another new flame retardant approach and the results will be presented in this paper. The objectives of the condensed phase study are (1) to understand condensed phase processes during burning of polymeric materials with and without flame retardant additives, (2) to develop a gasification model including thermal degradation chemistry and heat and degradation products transport processes, and (3) to characterize polymer melt-flow behavior and to be able to predict it quantitatively under well-defined conditions. The results in (1) and (2) will be briefly discussed in this paper and those in (3) will be presented by Dr. Ohlemiller in a separate paper. The objective of the study of gas phase modeling is to improve and extend our gas-phase model for the simulation of burning of commodity polymers with and without flame retardants in the Cone Calorimeter. Since this work was presented in detail at the last UJNR Meeting, no discussion of this subject will be given. The objective of the study to characterize polymer physical properties is to

evaluate the elastic, viscoelastic, and fracture properties of the new environmentally-friendly, flame retarded polymeric materials. Finally, the objective of the economic study is to provide an analysis of economic impacts of fire safe materials technology. The last two parts of the project, characterization of physical properties and economics of fire safe materials, are not discussed in this paper due to space limitations.

2. New Flame Retardant Principles

We continue to work with clay-nanocomposites and have formed a consortium to study flammability aspects of clay-nanocomposites for various polymers. Since this approach was presented at the last UJNR Meeting, another flame retardant approach using silica was investigated and is described in this paper. At first, the influence of silica material properties (morphology, surface area, silanol concentration, and surface treatment) on flame retardant effectiveness was determined by preparing silica/PP samples using silicas with very different characteristics. We used fused silica, fumed silica, and a high pore volume (2.0 cm^3/g) silica gel. These samples were prepared by hand mixing powdered PP with the various silicas, followed by compression molding. Table 1 shows the material properties of the four types of silica used. These silicas are very different, specifically in terms of their particle morphology, surface area, and level of silanol functionality. Figure 1 shows representations of the silica types.

Observation of the gasification of the unmodified PP sample in a nitrogen atmosphere first reveals melting of the sample surface at about 30 s after irradiation (incident radiant heat flux: 40 ±2 kW/m^2), followed by the appearance of several large isolated bubbles at the surface, at about 60 s. Continued melting of the sample with more large bubbles was observed at about 90 s. Vigorous bubbling started at about 120 s and the sample surface was covered by a foamy-froth of very small bubbles (very similar in appearance to that of a beer "head") at about 180 s. This can be seen in the top left image in Figure 2. Vigorous bubbling, and a foamy-froth, continued over the rest of the gasification experiment as seen in the middle of the top image in Fig. 2.

The digitized video images of the sample of PP with fused silica (mass fraction 10 %) are not shown in Figure 2; however, similar bubbling phenomena as that of the pure PP sample were observed up to about 200 s. At about 250 s, the surface layer appeared to be more viscous, and had many small bubbles bursting through a more viscous, frothy-foam surface layer. This behavior continued until about 500 s when the surface became solid-like. Scattered white powder was observed after the end of the test, and its weight was close to 10 % of the original sample weight.

The digitized video images of the sample of PP with hydrophobic fumed silica (mass fraction 10 %) are also not shown in Figure 2; however, the behavior was similar to that of the pure PP sample up to about 200 s, with vigorous bubbling but without foaming, or any frothy-foam layer. After about 200 s, the sample had large bubbles rising through a viscous layer. However, this layer still looked like a fluid. After 400 s, some solid-looking islands were observed, and this pattern remained until the end of test. Vigorous bubbling was observed between the islands.

For the sample of PP with silica gel (mass fraction 10 %) initial melting and bubbling phenomena were similar to the above three samples up to about 180 s, as seen in the left bottom picture in Figure 2. At about 180 s, the sample surface rapidly solidified and a crust-like layer formed. It appeared that this layer continued to thicken; the production of the evolved degradation products slowed significantly, as seen in the middle and right bottom images in Figure 2. It appeared that molten polymer below the crust was transported to the surface through the crust by capillary action. The mass of the residue at the end of the test (800 s) appeared to be a rigid crust instead of a powder, and was about 9% of the original sample mass. Although the color of the residue was light gray, it appears that no significant amount of carbonaceous char was formed by the addition of the silica gel. Behavior very similar to the PP/silica gel sample was also observed for the PP/hydrophilic fumed silica sample: except that the surface layer of the residue at the end of the test was very fluffy and white.

The measured mass loss rates of the five samples are shown in Figure 3. The uncertainty in the measured mass loss rate has 5 % relative uncertainty derived from 3 replicate runs of several representative samples. A sharp increase in mass loss rate after about 200 s is clearly seen for the pure PP sample. After 300 s, the mass loss rates of the modified samples decrease in the order: PP/fused silica > PP/ hydrophobic fumed silica > PP/silica gel > PP/hydrophilic fumed silica. However, the mass loss rates of all samples are nearly the same until about 220 s. Actually, the addition of the four silicas slightly increases the mass loss rate before 200 s. This could be due to increased absorptivity of the samples with respect to the incident thermal radiant flux due to the strong broad band absorption of the Si-O peak at about 1100 cm^{-1}, as described later. This tends to absorb the external radiation close to the sample surface, and thus heats the sample surface faster.

From the visual observations of the gasification experiments it appears that the melt viscosity of PP is significantly enhanced by the addition of silica. Both silica gel and hydrophilic fumed silica show the same thickening behavior; with hydrophobic fumed silica and fused silica showing only slight thickening. For the hydrophilic fumed silica the thickening is due to inter-particle hydrogen bonding; on the other hand, the thickening from silica gel can in part be due to this type of mechanism, but entanglement of the polymer in the large silica gel pores may also play a part in increasing the viscosity[1]. After the formation of the crust layer, molten polymer and degradation products may seep through the crust layer toward the surface by capillary action. However, this transport rate through the crust layer tends to be much slower than transport by bubble formation/movement through the much less viscous molten layer in the pure PP sample.

The same types of PP samples were tested in the Cone Calorimeter to examine the effect of each silica type (except for the hydrophilic fumed silica) on heat release rate and mass loss rate during burning. The heat release rate results are shown in Figure 4. The uncertainty in the heat release rate measurement is within ± 10% based on both accuracy of the oxygen analyzer used in the experiments and of heat release rate per unit mass of oxygen consumption used in the data analysis. Although the external heat flux used in the Cone Calorimeter was 35 kW/m^2, instead of 40 kW/m^2 as in the gasification device, the relative order of mass loss rate among the four samples is exactly the same as that shown

in Figure 3. Heat release rate and mass loss rate decrease in the order: pure PP > PP/fused silica > PP/ hydrophobic fumed > PP/silica gel. The above trends indicate that the flame retardant mechanism of silicas tends to be physical in nature, instead of chemical, and also in the condensed phase, instead of the gas phase. Similar results are also obtained with ethylene vinyl acetate, EVA[2].

The basis for the physical effect of silica may be due to the thermal properties of the silica-loaded crust layer. The thermal diffusivities of accumulated silica gel, and of PP, are estimated here. The thermal conductivity [3] of silica varies significantly depending on its porosity. For example, it is 0.015 W/mK for fumed silica, and 1.1 W/mK for fused silica. Here the thermal conductivity of silica gel is assumed to be close to that of fumed silica. The estimated thermal diffusivity of the silica gel is roughly 1×10^{-4} cm^2/s compared to 6×10^{-2} cm^2/s for PP. Although, the value for silica gel is estimated, it is clear that the thermal diffusivity of the silica loaded crust layer should be much less than that of PP. Furthermore, the insulating effect of this layer should improve as the test progresses. The thermal diffusivity of fused silica is about the same as that of PP; therefore we assume that the addition of fused silica to PP does not have any significant effect on the thermal diffusivity of PP.

The reduction in the transport rate of thermal degradation products through the molten polymer layer, due to an increase in melt viscosity by the accumulation of fused silica, could explain the difference in mass loss rate between PP and PP/fused silica, shown in Figure 3. However, since no crust-like layer forms via the accumulation of fused silica, the increase in melt viscosity appears to be much less than that from fumed silica or silica gel. The difference in mass loss rate between PP/hydrophilic fumed silica and PP/hydrophobic fumed silica, shown in Figure 3, is due to the greater increase in viscosity of PP melt by hydrophilic fumed silica as compared to hydrophobic fumed silica, and thus a greater reduction in the transport rate of the degradation products in PP/ hydrophilic fumed silica. Therefore, the silica gel flame retardant mechanism in PP appears to consist of two mechanisms: first, reduction in the transport rate of the thermal degradation products; and second, reduction in thermal diffusivity of the sample near the surface due to gradual accumulation of silica gel, which acts as a thermal insulation layer. This is also true for fumed silica. The reduction in the transport rate of the degradation products is achieved by dramatically increasing the viscosity of PP melts due to hydrogen bonding of hydroxyl groups of silanols, and entanglement of polymer chains with the large pores of silica gel. This transport mechanism tends to dominate early in the test, because a small amount of silanol increases melt viscosity dramatically [1], but the insulation mechanism requires a relatively large accumulation of fumed silica, or silica gel, for the layer to become an effective insulator.

3. Condensed Phase Processes

A condensed phase model is being developed as a part of an overall model to describe the burning behavior of thermoplastics in the Cone Calorimeter. A one-dimensional model has been developed to describe the bubbling behavior of thermoplastic materials exposed to a high heat flux and the effects of these bubbles on thermal and transport properties.

The geometry treated by this model is a horizontal sample of specified initial thickness resting on a non-reactive substrate that satisfies adiabatic thermal conditions at its lower surface. A specified radiant heat flux is applied from above, with losses occurring at the surface of the polymeric sample due to radiation, convection, and reflection. As the temperatures within the sample and substrate rise, the polymer begins to decompose into gaseous components. This model focuses its attention on the finite-rate transport of these gases to the sample surface and on the effects of gases contained within the sample on its thermal behavior and mass loss rate.

The one-dimensional bubble model is based on finite element theory. The sample is divided into a large number of elements in the direction perpendicular to the heated surface, with elements bounded by nodes. Initially, the thicknesses of all elements are identical, and a bubble of zero size is located at the midpoint of each element. The external heat flux is applied, and the nodal temperatures at the next time step are determined by standard finite element techniques. During each timestep, gasification takes place within each element. The amount of gas generated during the timestep is determined by integrating an Arrhenius expression over the element thickness. The gas is then apportioned to one or more bubbles located within the element.

At this point in the calculation, each bubble is represented by a one-dimensional gas layer, whose increase in thickness is linked to a decrease in polymer layer thickness by mass conservation and the ratio of gas density to polymer density. To determine the movement of this gas, the thickness of the bubble and its growth rate are converted to an equivalent radius and radial growth rate. Stokes flow calculations of bubble velocity due to viscosity gradients, surface tension gradients, and buoyancy now relocate each bubble within the sample. If a bubble touches the upper surface, it is considered to have "burst." The sum of the masses of gas from all bubbles that have burst during this timestep determines the current mass loss rate. These bubbles are removed from further calculations. If any element is left without a bubble after the bubbles are moved, a new bubble of zero size is located at its midpoint.

The volume fractions of gas and polymer can now be computed in each element from comparison of the thicknesses of gas layers (bubbles) whose centers are located within the element to the thickness of the remaining polymer. The total element thicknesses and the locations of nodes are also adjusted. The volume fractions combine with material properties of the gas and polymer to determine the equivalent thermal conductivity, density, and specific heat of each element, and element velocities are calculated from the motion of polymer and gas during this timestep.

The attached figures show the mass loss rate, Figure 5, and a time sequence of the bubbling sample, Figure 6, that result from this numerical procedure for a sample of polypropylene. The cross-sectional area of the computational space is determined by the bubble number density, and bubbles are assigned a random location in the horizontal direction for visualization purposes during this time step. The next finite element calculation of temperature is now performed. This procedure continues until the polymer has completely gasified.

References

[1] R.K. Iler, The Chemistry of Silica, John Wiley & Sons, New York, p. 588 (1979).

[2] J.W. Gilman, T. Kashiwagi, M. Nyden, and R.H. Harris,"New Flame Retardants Consortium: Final Report. Flame Retardant Mechanism of Silica" NISTIR 6357, June 1999.

[3]" CAB-OSIL Untreated Fumed Silica Properties and Functions" Cabot Corp. TD-100, May(1997).

[4] G. Wypych, Handbook of Fillers, 2nd Edition, Chemical Technology Publishing, Toronto, Canada, Chapter 2, 1999.

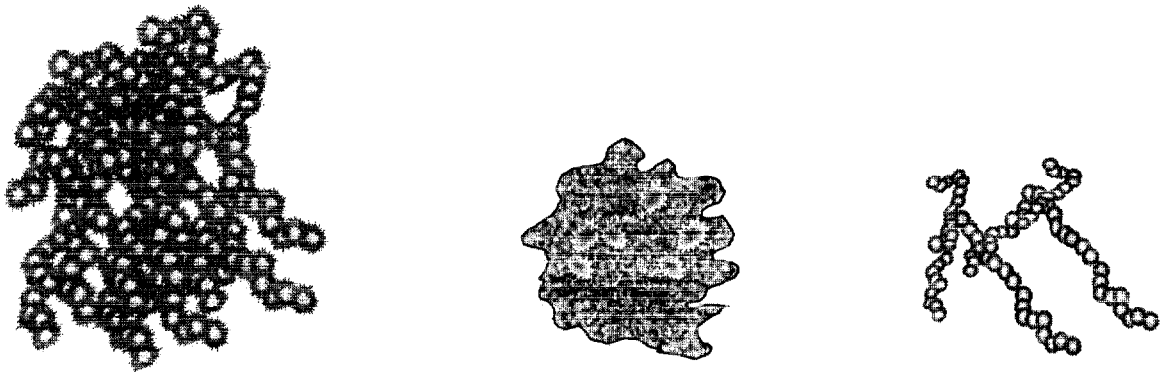

Figure 1. Drawing representing the different silica-morphologies for silica gel (left), fused silica (center), and fumed silica (right).

Table1 1. Material properties of various silicas.

Silica	Porosity (cm^3/g)	Thermal Treatment (°C, h)	Silanol Density ($SiOH/nm^2$)	Surface Area (m^2/g)	Particle size (μm)
Fused Silica amorphous	~ 0	100 °C 2h	low	low	7
Fumed Silica hydrophilic	NA	None	3 - 4	255 ± 25	aggregate length 0.2 – 0.3
Fumed Silica hydophobic[a]	NA	100 °C 15h	1 - 2	140 ± 30	" "
Silica Gel	2.0	900 °C 15h	0.4	400 ± 40	17

a: ~ half of the SiOH groups are capped by trimethysilylation [4].

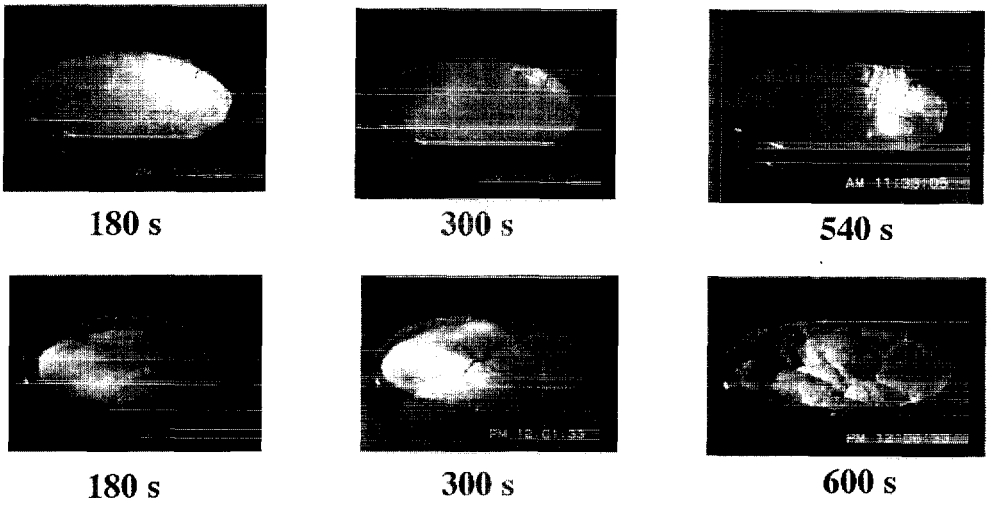

Figure 2. Digitized images of sample surface during gasification in N_2 at 40 kW/m^2. Pure PP (top row); PP with silica gel (mass fraction 10%) (bottom row).

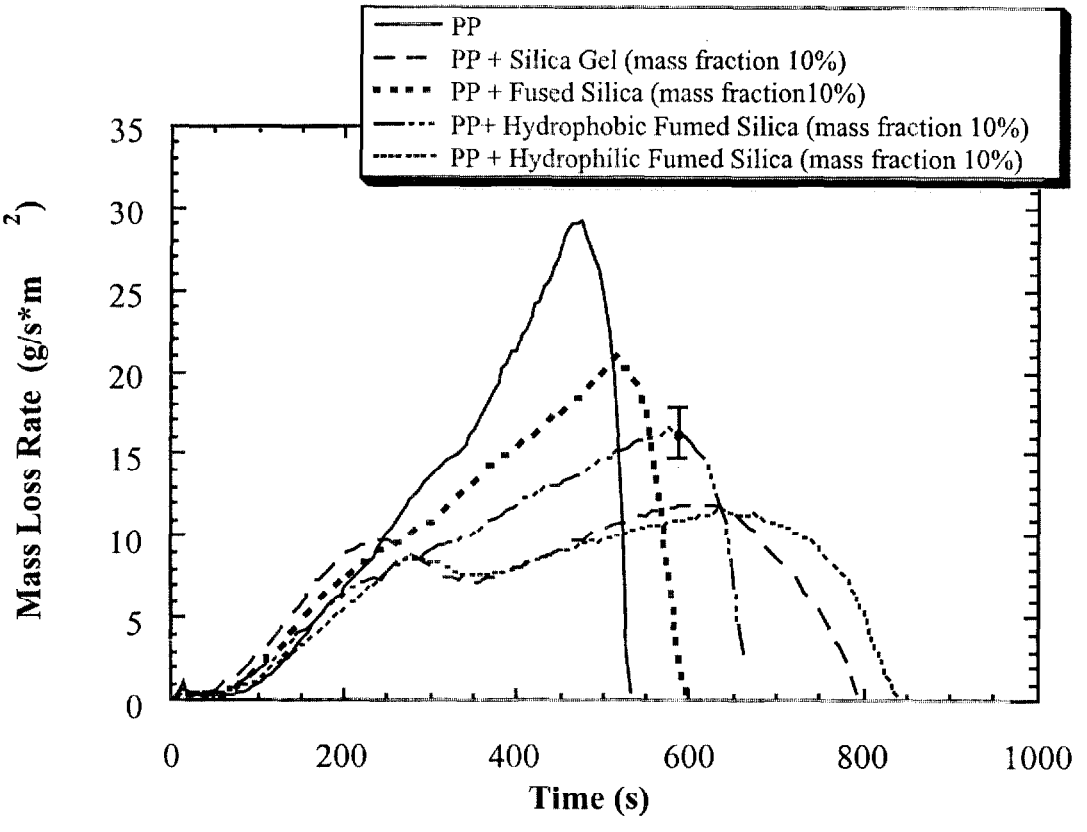

Figure 3. The mass loss rate data from the gasification (N_2 at 40 kW/m^2) of: pure PP, PP/silica gel, PP/fused silica, PP/hydrophobic fumed silica, and PP/hydrophilic fumed silica. This shows the effect of silica type on the gasification rate of PP.

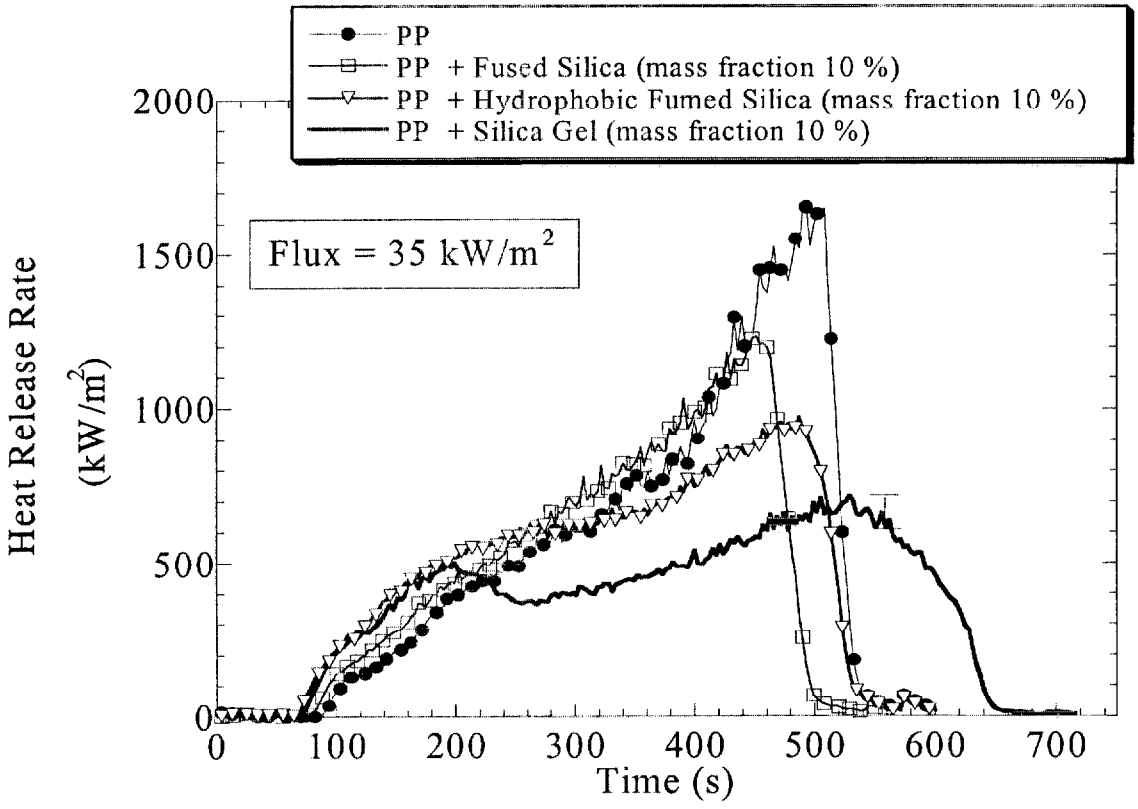

Figure 4. Effects of the addition of various silicas on heat release rate of PP

Reference

[1] R.K. Iler, The Chemistry of Silica, John Wiley & Sons, New York, p. 588 (1979).
[2] J.W. Gilman, T. Kashiwagi, M. Nyden, and R.H. Harris,"New Flame Retardants Consortium: Final Report. Flame Retardant Mechanism of Silica" NISTIR 6357, June 1999.
[3]" CAB-OSIL Untreated Fumed Silica Properties and Functions" Cabot Corp. TD-100, May(1997).
[4] G. Wypych, Handbook of Fillers, 2nd Edition, Chemical Technology Publishing, Toronto, Canada, Chapter 2, 1999.